Tuijin Jishu/Journal of Propulsion Technology
ISSN: 1001-4055
Vol. 45 No. 1 (2024)

Modification of USBR Type III Stilling Basin Using a Stepp Stair Model to Improve Hydraulic Performance and Energy Dissipation Effectiveness

Gilang Idfi[1*], Umboro Lasminto[2] , Anak Agung Gde Kartika [3]

[1]Faculty of Civil, Planning and Geo-Engineering, Institut Teknologi Sepuluh Nopember, 60111, Surabaya, Indonesia

ABSTRACT

This research examines common problems in open and closed transition channels, including hydraulic instability due to changes in channel shape that cause cross flow at constrictions or widenings. Closed channels experience turbulence at the outlet, require additional blocks to balance the flow, and can cause damage in downstream rivers due to suboptimal energy absorbers, requiring annual maintenance. Energy dissipators handle energy loss due to elevation differences. The research method involved modeling and testing at the ITS Water Resources and Ocean Engineering Laboratory with several alternatives. The results show that the ratio of Y2 and Y1 and the hydraulic jump length affect the efficiency of the stabilization pond. In the study, the negative Stepp stair model had an energy dissipation ratio of 67.30% and an efficiency of 32.70%. The water level test on the USBR III model shows the difference in elevation between the USBR type and the Stepp stair. The USBR III Stilling Basin had the lowest elevation of +1.65 and the highest of +16.95, while the Stepp stair model had the lowest elevation of +1.65 and the highest of +17.95. The velocities of the Stepp stair model are in a lower range than the USBR Type III Stilling Basin model. The velocities in the USBR Type III model ranged from 19.17 m/s to 29.80 m/s, while those in the Stepp Stair model ranged from 17.42 m/s to 28.14 m/s. If this model is applied later, it will reduce erosion symptoms downstream of the stilling basin due to lower velocities.

Keywords USBR, Energy Dissipator, Stepp Stair, Hydraulic Jump

INTRODUCTION

One of the essential components of a dam structure is the spillway (Aditya et al., 2021). The Spillways are used in dams as energy dissipators (Daneshfaraz et al., 2022; Jayant et al., 2023). The spillway serves to overcome excess water in the reservoir, preventing water from overflowing over the dam's crest, which could potentially endanger the building structure (Li et al., 2019). This structure reduces the energy of the supercritical flow of the channel (drop line) into the subcritical flow to return to the river (Qin et al., 2020; Bantacut et al., 2022). In the design of a spillway, flow capacity and energy dissipation are two aspects that need to be considered (Prasetyorini & Priyantoro, 2015). Flow capacity refers to the ability to convey water safely and by hydraulic principles in the spillway channel. When water overflows the spillway, it flows into the spillway channel and an energy dissipator called the stilling basin (Babaali et al., 2015). The spillway consists of several parts: the crest spillway, transition channel, launcher channel, energy dissipator, and downstream guide channel. Problems often

occur in spillway systems related to transition channels, launcher channels, and energy dissipators (Mansoori et al., 2017).

Problems that often occur in transition channels can appear in both open and closed channels. In open channels, the problem occurs in changes in the shape of the channel bottom, where the narrowing and widening result in cross-flow (Rohmanto et al., 2021). The result of the irregular hydraulic performance of the transition channel is unstable conditions downstream. In a closed channel, the turbulence of the flow results in two cross-flows at the outlet, requiring the addition of a block at the bottom of the channel (Valero et al., 2016).

The flow phenomenon in the launch channel involves high-speed flow with supercritical conditions. Before conveying the flow to the river, it must be damped through energy dissipators to convert it to subcritical flow (Ulfiana, 2018). A common problem is damage to the downstream river due to energy dissipators not functioning optimally, requiring maintenance almost yearly (Zulfan, 2017). The main objective is to achieve subcritical flow conditions in the downstream river to avoid damage to the original riverbed. The function of energy damping is to accommodate energy losses that occur due to elevation differences in building structures (Noverdo et al., 2021). Energy dissipators are designed to reduce the kinetic energy at the foot of the spillway (chute) before it goes into the original river. During the dissipation process, the phenomenon of hydraulic jump appears, indicating the dissipation process (Hagel, 1992; Bahmanpouri et al., 2023), in which height planning is associated with the need for downstream water depth of the energy reducer. volume (water depth behind) (Ibrahim et al., 2022; Elnikhely & Fathy, 2020). The hydraulic jump can also be controlled or directed by the existence of an end sill to complete downstream dissipation (Vayghan et al., 2023; Tiwari & Goel, 2014). The history of research on energy absorbers has been carried out by several previous researchers, namely Bradley & Peterka (1958), Hager (1992), dan Chanson (2000), In general, energy absorbers can be classified into four categories: (i) rock energy absorbers; (ii) stilling basins; (iii) plunge pools; and (iv) free jets (Barjastehmaleki, 2015).

Determining the four types of energy dissipators is based on geological conditions and natural riverbed materials. River conditions with a bed consisting of hard rock are suitable for using free jets or plunge pool-type energy dissipators because the dampened flow will be emitted back into the river (Pamungkas, 2014). The hydraulics formula used as the basis for planning energy dissipators is derived from the principle of the law of energy conservation and the phenomenon of forces acting on the cross-section for flow conditions that change from supercritical to sub-critical flow (Sasra Olga Pandani et al., 2022). Energy absorbers widely used as a basis for planning are generally stilling basin-type energy dissipators. The principle of a stilling basin-type energy dissipators occurs due to friction or collision between water molecules, so water circulation occurs in the energy reducer (Suroto Budinetro et al., 2010).

Several design standards for the shape of energy absorbers have been developed, including Saint Anthony Falls (SAF Basin), The United States of Berau Reclamation (USBR), Bhavani Basin, The Institute of Hydraulics Vedeneev (VNIIG) Lanigrade (USSR), and The United States Corps of Engineers (USCE).

Based on several studies conducted, the condition of the water depth downstream (tail water depth) dramatically

affects the effectiveness of damping. The minimum water depth that must be available is 0.8 conjugation depth (y2) for USBR type III (Wahl & Falvey et al., 2018), if it is less than the minimum depth, then there is no dissipation effectiveness because of the jumps that occur out of the stilling basin (Gebhardt et al., 2018; Hassanpour et al., 2021). To preserve the river geometry's integrity, it is crucial to guarantee the occurrence of hydraulic jumps in the stilling basin (Soori et al., 2017; Bhate et al., 2021). When the tailwater depth does not meet the requirements, a negative (adverse) pool slope is required to reduce dissipation energy and raise the downstream water level. The negative (adverse) slope also serves to minimize pulsating wave symptoms. This study uses a stepped adverse stilling basin to increase the hydraulics performance, so the flow conditions with high velocity are expected to be perfectly damped with this model (Zulfan et al., 2022).

RESEARCH METHODS

Hydraulics Characteristics of a Spillway

The spillway building requires that when the flood discharge flows, there is no backwater. To meet these requirements, the spillway building is planned so that when flowing flood discharge, the difference in water surface elevation upstream and downstream of the regulating weir is not less than 2/3 times the water level above the spillway (Kurniawan & Siregar, 2022).

Flow Profile

There are generally three flow profile calculation methods: the graphical integration method, the direct integration method, and the phasing method. The phasing method is expressed by dividing the channel into short sections and then calculating in stages from one end to the other. Several phasing methods exist, but only some of the best methods exist for every problem (Kurniati et al., 2019).

The Direct Stages Method is a simple method that can be used for prismatic channels. The equation used (Hendratta & Tangkudung, 2020):

$$S_0 + \Delta_o + h_1 \propto_1 \frac{V_1^2}{2g} = h_2 + \propto_2 \frac{V_2^2}{2g} + Sf\Delta f \quad \text{.....(1)}$$

$$\Delta_x = \frac{E_2 - E_1}{So - Sf} = \frac{\Delta E}{So - Sf} \quad \text{.....(2)}$$

While $E_1 = E_2 = E$, so:

$$E = h + \alpha \frac{v^2}{2g} \quad \text{.....(3)}$$

Where :

E = specific energy (m)

h = water depth (m)

V = average velocity (m/s)

So = channel bottom slope

Normal depth (y) is the depth of water occurring in the channel obtained from the uniform flow equation. Manning's equation is used to calculate depth and flow velocity. As is well known, calculations for flow through open channels can only be done using empirical formulas, one of which is the Manning equation, which is relatively practical, and the results are quite satisfactory in its application, as in the following equation. (Putro & Hadihardaja, 2013):

$n = 1/v.\ R^{2/3}.S^{1/2}$……...(4)

Where :

n = manning's coeficient value

v = velocity in the channel (m/s)

S = channel bottom slope

Hydraulic Jump

Hydraulic jump is the rapid state from supercritical flow to subcritical flow. The water level increases suddenly and there is a significant loss of energy during the hydraulic jump. Hydraulic jump occurs when water changes rapidly from supercritical flow to subcritical flow, resulting in a sudden increase in water level and significant energy loss [41]. The beginning of the jump is marked by the formation of a turbulent vortex, which draws energy from the main flow and subsequently fragments into smaller parts downstream [42]. A significant turbulent vortex is formed at the beginning of the jump. This vortex draws energy from the main flow and the vortex fragments into smaller parts while flowing downstream (Pamungkas, 2014). For supercritical flow in a horizontal rectangular channel, the flow energy will be suppressed by the frictional resistance of the channel, resulting in a reduction in velocity and an increase in height in the flow direction. The nature of the flow downstream and the energy lost in the hydraulic jump can be deduced from the momentum principle as a function of the Froude number upstream and the depth of flow upstream. Normal depth (y) is the depth of water occurring in the channel obtained from the uniform flow equation. For the calculation of depth and velocity of flow, Manning's equation is used.

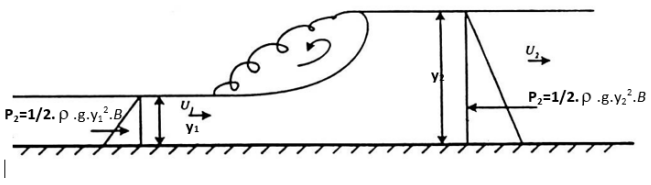

Figure 1. Momentum Equation in Hydraulic Springboard

In hydraulic springboard events, the fundamental component that affects the energy calculation is the momentum equation:

$P1 - P2 = \rho Q(v1 - v2)$ ……(5)

$\left(\frac{1}{2}\rho g {y_1}^2 - \frac{1}{2}\rho g {y_2}^2\right) B = \rho u_1 y_2 (y_1 - y_2)$……(6)

(y1-y2)(y1+y2) = $\frac{2u1y1}{g}(u2 - u1)$ ……...(7)

While from the continuity:

Sq = v1.h1 = v2.h2

By combining the above equations then:

(y1+y2) = $\frac{2v1^2}{g}\frac{y1}{y2}$ ……..…… (8)

$\frac{y_2}{y_1}\left(1 + \frac{y_2}{y_1}\right) = 2({F_1}^2)$ ……..……(9)

Then the above equation is simplified to get an estimate of the depth of flow after the hydraulic jump, the following equation is obtained:

$\frac{y_2}{y_1} = \frac{1}{2}\left(\sqrt{1 + 8{F_1}^2} - 1\right)$ ……..……..(10)

Because y1 is the depth before the hydraulic jump and y2 is the depth after the hydraulic jump. Hydraulic jump that occur on a horizontal bed are of several different types. According to research conducted by the United States Bureau of Reclamation, hydraulic thrust can be distinguished based on the Froude number Fr1 of the flow involved. The hydraulic surges that occur on a horizontal bed are as follows (Yusuf & Wibowo, 2013):

1. Critical Flow :

For Fr1 = 1 critical flow occurs, so that no jumps can be formed.

2. Choppy Jumps

For Fr1 = 1 to Fr1 = 1,7 choppy jump that occurs with ratio y2/y1 is 1 to 20.

3. Weak Jumps

For Fr1 = 1.7 to Fr1 = 2.5, a series of pulsating wave form on the jump surface but the downstream water surface remains calm. The overall speed is uniform and the energy loss is low. The ratio y2/y1 varies from 2 to 3.1.

4. Oscillating Jumps

For Fr1 = 2.5 to Fr1 = 4.5, the oscillating rays accompany the jumping platform and move towards the surface and return without a definite period. Each oscillation creates a large irregular wave and causes infinite damage to the embankment. The ratio y2/y1 varies from 3.1 to 5.9.

5. Steady Jump

The downstream surface's edges curl and the point with the highest burst velocity tends to diverge from the flow between Fr1 = 4.5 and Fr1 = 9. These two occurrences typically take place on the same vertical surface. The movements and surges that occur are not greatly influenced by the bottom water depth. The hydraulic jump is very balanced, which is the best characteristic. The energy dissipation is 45%-70%. The y2/y1 ratio ranges from 5.9 to 12.

6. Strong Jump

For Fr > 9 and above, high burst speeds separate the rolling wave from the pedal face, giving rise to a downstream wave. If the surface is rough, it will affect the waves generated. Jump moves are rare but effective as the energy reduction can reach up to 85%. The ratio y2/y1 is greater than 12.

Bradley dan Peterka (Bradley & Peterka, 1958) classifies hydraulic jumps in four groups, namely (Hager, 1992):

1. Pre-jump, if 1.7 < Fr1 < 2.5.

2. Transition jump, if 2.5 < Fr1 < 4.5.

3. Stabilised-jump, if 4.5 < Fr1 < 9.

4. Choppy jump), if Fr1 > 9.

Hydraulic jumps based on position relative to the foot of the channel slope angle, i.e. (Hager, 1992).

1. A-jump, occurs if the start of the jump occurs exactly at the foot of the angle of inclination of the channel

2. B-jump, occurs between jump A and jump B.

3. C-jump, occurs if the start of the surge occurs at the channel slope and the end of the water wave roll occurs exactly at the foot of the channel corner.

4. D-jump, occurs if all the surges occur on the channel slope, both the beginning of the jump and the end of the surge which is the end of the surge.

Other forms of hydraulic stepping include hydraulic stepping in non-rectangular channels, such as trapezoidal channels, circular channels, triangular channels, and profil U-shaped channels, and submerged hydraulic stepping (Hager, 1992).

Energy Dissipator

The flow phenomenon in the launch channel is characterized by a very high flow velocity and supercritical flow conditions. Therefore, before the flow of water has flowed into the river, it must be slowed down and changed to sub-critical flow conditions so that scouring does not occur, which worsens the geometry of the river at the bottom and riverbanks (Dara Lufira & Marsudi, 2015).

Frame Of Mind

To conduct this investigation, a physical model of a USBR Type III stilling basin was constructed. Three circuit breakers are located in the Type III USBR stilling basin: an end platform is located downstream, a baffle block is located in the middle, and a trough block is located upstream in the tank. In order to lower the flow rate from the initial supercritical flow to a subcritical rate, these three stilling basin sections work to forecast or minimize the flow energy.

Ten flow variations were used in this experiment, and the flow slipped straight into the basin downstream of the canal and returned to the reservoir without the need to erect a barrier as a wastewater regulating device downstream of the canal. The critical depth (yc), flow rate along the spillway (v), flow depth (d1) prior to and following the hydraulic leap (d2), and step length hydraulic jump (Lj) were all measured during the testing of each model.

Measurement devices, such as Thompson gauges, pitot tubes, flow meters, acoustic Doppler velocimeters (ADVs), and current meters, are used to record flow and velocity in order to facilitate flow control and ensure data gathering accuracy. As seen in Figures 1a and 1b, the measurement structure utilized in this work is a triangular spike dam, Thompson dam, or V-notch, with each side of the triangle measuring 35 cm in length. The investigation employed a range of flow rates, from 6.124 to 30.546 lt/dt. The threshold base is positioned horizontally to reduce the speed of the inflow, and the measuring building is positioned to prevent flow. Figure 2 shows where each measuring device is located.

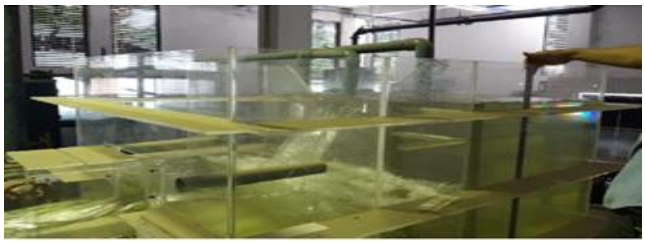

Figure 1a. Thompson Weir Measuring Instruments/V-Notch

Figure 1b. Flow Velocity Measurement with Current Meter

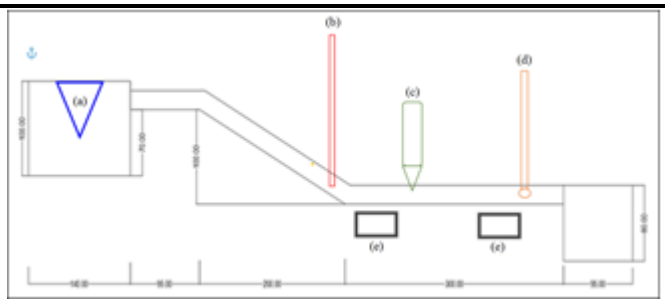

Figure 2. Schematic of Measuring Instrument Placement (a) Thompson Measuring Instruments / V-Notch, (b) Pitot Pipes, (c) Acoustic Doppler velocimetry (ADV), (d) Current Meter, (e) Cameras

Second Variation Method With Tailwater Effect

The second option involves analyzing the initial model by considering the influence of water level at the downstream boundary condition, commonly referred to as downstream water depth. During the test, each change in flow rate also changes the position of wastewater depth.

The height of wastewater depth is adjusted up or down until the effect of depth is no longer present.wastewater. The depth of the wastewater can affect the damping efficiency (ΔE) due to the backwater effect. In addition to the parameters of the first alternative, data on the height of the wastewater (y3/tw) and damping efficiency (ΔE) of the second alternative are also obtained.

In this second alternative, An acrylic barrier of the same height as Y2 was used downstream of the channel to create the desired effluent effect. Based on a number of conducted studies, downstream water depth conditions (downstream water depth) greatly affect the damping efficiency. The minimum water depth required is 0.8 conjugate depth (y2). The shape and dimensions of the barrier block can be seen in Figure 3

Figure 3. Barrier Block at Downstream Flume

Observing hydraulic parameters due to the influence of Tailwater begins with observing the water depth value upstream of the stilling basin (Y1) at the foot of the discharge channel up to the water depth value d downstream of the stilling basin (Y2). Documentation of the measurement implementation can be seen in Figure 4.

Figure 4. Testing Process Documentation

Velocity Conditions in Turbulent Areas

The turbulent zone, or more specifically, the vicinity of the baffle block, is where velocity testing is carried out, situated between the trough block and the end threshold. There is a sudden shift in flow as the launch channel's sharp slope changes to the stillation tank's mild slope. often referred to as rapid flow change. This situation causes chaos in the current conditions. This flow is characterized by abrupt velocity fluctuations, unpredictable flows, and irregular patterns. The speed recording value in this test is produced automatically by the Acoustic Doppler Velocity Meter (ADV). Figures 5a and 5b show an example of a test document for a flow rate of 10.1 liters/s.

Figure 5a. Turbulen Condition

Figure 5a. Velocity Testing Using ADV

RESULTS AND DISCUSSION

USBR Type III Model with Tailwater Effect

Stilling basin performance assessment parameters, essential benchmarks in evaluating the effects that occur, can be measured by considering two key aspects: relative loss value (ΔE/E1) and efficiency (E2/E1).

The relative loss value (ΔE/E1) shows the change in stilling basin efficiency compared to the initial value (E1). This shows how specific factors, such as temperature or water composition changes, affect the pool's

performance. Meanwhile, efficiency (E2/E1) is a parameter that provides information about the extent to which stilling ponds can maintain their effectiveness in fulfilling specific goals, such as maintaining water quality or supporting aquatic life. Details of the calculation of these two parameters can be explained further and are found in Table 1 and Table 2.

Table 1. Hydraulic Parameter Calculation (a)

No	Discharge (cm^3/s)	Y1 (cm)	V1 (cm/s)	Fr1	Y2 (cm)	y2/y1
1	3818	9.70	272.71	10.41	9.96	14.23
2	4340	0.80	271/25	9.68	10.56	13.20
3	4900	0.85	288.24	9.98	11.58	13.63
4	5510	0.95	290.00	9.50	12.30	12.94
5	6155	1.05	293.10	9.13	13.05	12.42
6	6850	1.15	297.83	8.87	13.86	12.05
7	7700	1.25	308.00	8.80	14.94	11.95
8	8360	1.40	298.57	8.06	15.27	10.90
9	9200	1.55	296.77	7.61	15.93	10.27
10	10100	1.65	306.06	7.61	16.95	10.27

Table 2. Hydraulic Parameter Calculation (b)

No	Discharge (cm^3/s)	Lj (cm)	E1 (cm)	E2 (cm)	ΔE	Energy Dissipation Ratio	Efficiency
1	3818	9.70	38.61	10.15	28.46	73.72	26.8
2	4340	0.80	38.30	10.78	27.52	71.86	28.14
3	4900	0.85	43.19	11.81	31.38	72.66	27.34
4	5510	0.95	43.81	12.55	31.26	71.35	28.65
5	6155	1.05	44.83	13.33	31.50	70.27	29.73
6	6850	1.15	46.36	14.17	32.19	69.44	30.58
7	7700	1.25	49.60	15.27	34.33	69.20	30.80
8	8360	1.40	46.84	15.65	31.19	66.59	33.41
9	9200	1.55	46.44	16.35	30.09	64.79	35.21
10	10100	1.65	49.39	17.40	32.00	64.78	35.22
Average						**69.47**	**30.53**

Detailed analysis in Table 1 reveals that the average energy dissipation ratio in the USBR Type stilling basin, which is influenced by tailwater, reaches 69.47%, while the efficiency level is 30.53%. This information provides a comprehensive picture of how effective USBR-type stilling basins are in managing and dispersing

energy, especially when considering the influence of tailwater. The relationship between relevant and significant parameters is illustrated through the graphs in Figures 6 and 7.

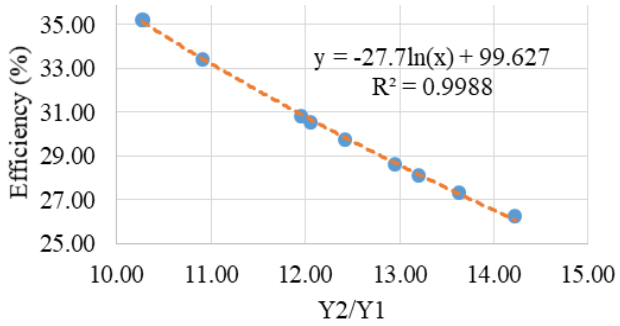

Figure 6. Efficiency and Y2/Y1 Relationship Graph

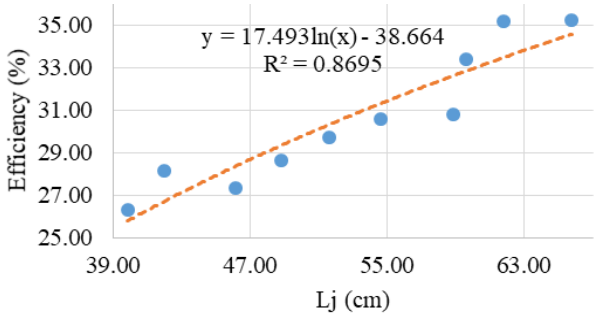

Figure 7. Efficiency and Lj Relationship Graph

Efficiency is negatively correlated with the comparison of Y2 and Y1 values; figure 4 illustrates this relationship. The smaller the difference between Y2 and Y1 values, the lower the stilling basin's performance efficiency.

Figure 5 illustrates how the length of the hydraulic jump (Lj) and the required stilling basin dimension cause the efficiency to drop. It is possible to read this as an inverse relationship between the stilling basin's efficiency and the value of Lj.

Negative Stepp Stair Model With Tailwater Effect

The process of observing hydraulic parameters, which are influenced by tailwater, is initiated by recording water depth values starting from the upstream part of the stilling pool, identified as Y1, and continuing the recording down to the downstream part of the stilling pool, symbolized as Y2. The documentation process for implementing this measurement is detailed in Figures 8a and 8b.

This approach allows comprehensive recording of changes in water depth from the beginning to the end of the stilling basin, helping to identify patterns and trends that may arise due to the influence of tailwater.

Figure 8a. Documentation of Negative Stepp Stair Testing With Tw

Figure 8b. Documentation of Negative Stepp Stair Testing With T

The performance assessment parameters of the influenced stilling basin can be measured from the relative loss ratio (ΔE/E1) and efficiency (E2/E1). The calculation of these parameters can be seen in table 3 and table 4 below:

Table 3. Hydraulic Parameter Calculation (a)

No	Discharge (cm^3/s)	Y1 (cm)	V1 (cm/s)	Fr1	Y2 (cm)	y2/y1
1	3818	0.70	272.71	10.41	10.96	15.65
2	4340	0.80	271,15	9,68	11.56	14.45
3	4900	0.85	288.24	9,98	12.58	14.80
4	5510	0.95	290.00	9,50	13.30	14.00
5	6155	1.05	293.10	9.13	14.05	13.38
6	6850	1.15	297.83	8.87	14.86	12.92
7	7700	1.25	308.00	8.80	15.94	12.75
8	8360	1.40	298.57	8.06	16.27	11.62
9	9200	1.55	296.77	7.61	16.93	10.92
10	10100	1.65	306.06	7.61	17.95	10.88

Table 4. Hydraulic Parameter Calculation (b)

No	Discharge (cm^3/s)	Lj (cm)	E1 (cm)	E2 (cm)	ΔE	Energy Dissipation Ratio	Efficiency
1	3818	44.11	38.61	11.11	27.49	71.21	28.79
2	4340	46.28	38.30	11.74	26.56	69.34	30.66

3	4900	50.44	43.19	12.77	30.42	70.43	29.57
4	5510	53.09	43.81	13.52	30.30	69.15	30.85
5	6155	55.88	44.83	14.29	30.54	68.13	31.87
6	6850	58.94	46.36	15.13	31.23	67.37	32.63
7	7700	63.15	49.60	16.23	33.37	67.27	32.73
8	8360	63.93	46.84	16.60	30.23	64.55	35.45
9	9200	66.12	46.44	17.30	29.14	62.74	37.26
10	10100	70.07	49.39	18.35	31.04	62.85	37.15
Average						**67.30**	**32.70**

It can be seen in table 3 and table 4 that the average energy dissipation ratio of the negative stepp stair with the influence of tail water is 67.30% while its efficiency is 32.70%. The relationship between parameters is presented in the graphs in figure 9 to figure 11 below:

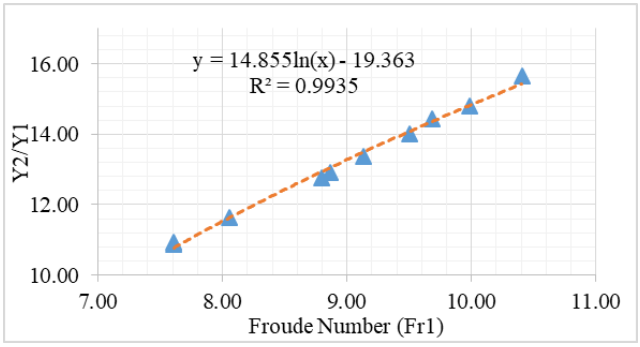

Figure 9. Relationship Graph of Y2/Y1 and Fr1

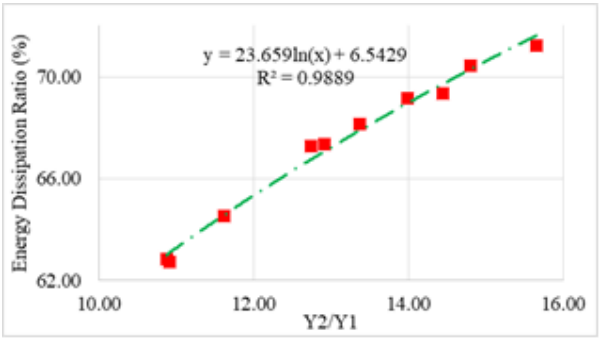

Figure 10. Relationship Graph of Y2/Y1 and Energy Dissipation Ratio

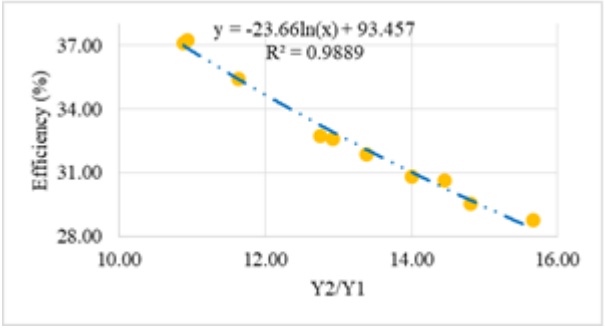

Figure 11. Graph of Y2/Y1 Relationship and Efficiency

The association graph between Y2/Y1 and FR1 is displayed in Figure 9. The value of FR1 that occurs increases with the difference between Y2 and Y1. The energy dissipation ratio's value is determined by the difference between Y1 and Y2. As illustrated in figure 10, the energy dissipation ratio increases with the ratio between Y2 and Y1. The efficiency is negatively correlated with the comparison of Y2 and Y1 values; as figure 11 illustrates, the stilling basin's performance efficiency will decrease as Y2 and Y1 values diverge further.

Comparison of USBR Type III and Negative Stepp Stair

Comparative observations of the USBR type III and the negative stepped stair also the calculation of these parameters can be seen in the following figure:

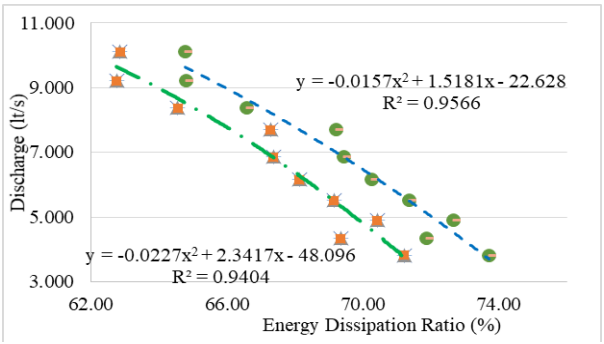

Figure 12. Energy Dissipation Ratio Graph of USBR Type and Negative Stepp Stair

Where:

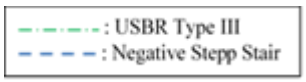

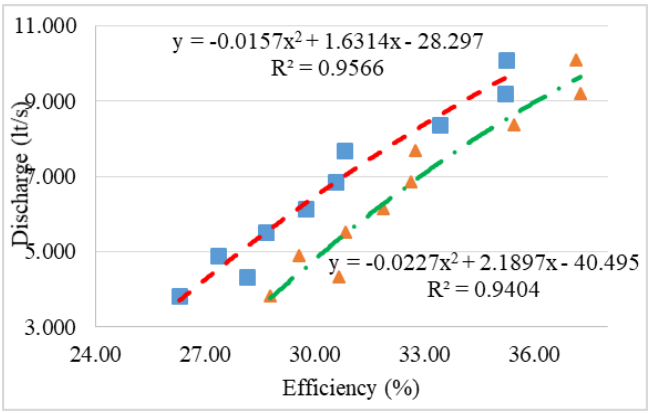

Figure 13. Efficiency Graph of USBR Type III and Negative Stepp Stair

Where:

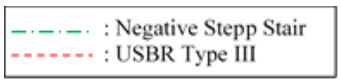

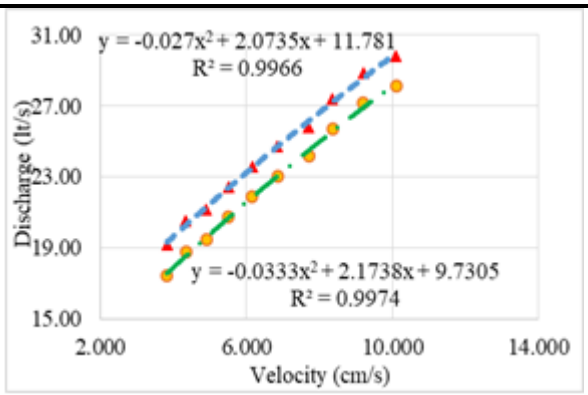

Figure 14. Velocity Chart of USBR Type III and Negative Stepp Stair

Where:

: Negative Stepp Stair
: USBR Type III

It can be seen in figure 12 that the dissipation ratio produced by the model of negative stepp stair is more optimal in reducing flow energy than the USBR Type III model Table 1 further displays the average energy dissipation ratio generated by USBR Type III, which is 69.47%. Table 2 shows the energy dissipation ratio multiplied by the negative stepp stair model, which is 67.30%, so it can be interpreted that the model of the negative stepp stair can increase the energy reduction performance by 2.17%.

The efficiency value will always be inversely proportional to the ratio of the energy dissipation value. In figure 13, the efficiency generated by the model of the negative stepp stair is greater than that of the USBR Type III model. It can also be seen in Table 1, where the average efficiency produced by USBR Type III is 30.53%, while in Table 2, it can be seen that the efficiency produced by the model of the negative stepp stair is 32.70%, so it can be interpreted that the model of negative stepp stair can increase efficiency by 2.17%.

By applying the model of the negative stepp stair, the value of the flow velocity that occurs can be reduced; this can be seen in figure 14, the velocity and discharge graph, where the value of the velocity of the negative stepp stair is below the USBR Type III model. The velocity in the USBR Type III model is 19.17 m/s–29.80 m/s, while in the negative stepp stair, it is 17.42 m/s–28.14 m/s. So it can be concluded that if this model of the negative stepp stair is applied, it will reduce the symptoms of erosion downstream of the stilling basin due to the density that occurs.

A comparison of the resulting water level elevation when the flow occurs in the USBR Type III stilling and the negative stepp stair stilling basin can be seen in the following figure 15:

Where:

: Negative Stepp Stair
: USBR Type III

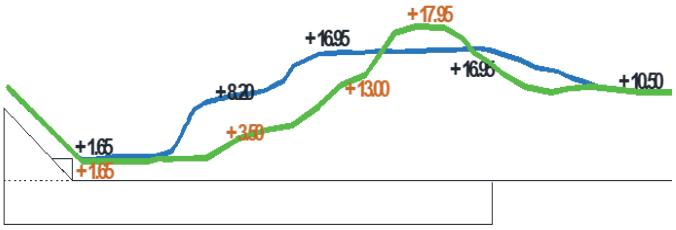

Figure 15. Comparison of Water Level Profiles in USBR Type III and Negative Stepp Stair

The USBR Type III stilling basin (blue line) has the lowest water level elevation of +1.65 and the highest water level elevation of +16.95, with a downstream water level elevation of +10.50, as shown in figure 15. On average, the negative stepp stair produces a water level elevation of +1.65 and the highest is +17.95, with a downstream water level of +10.50. The condition of the water level in the the negative stepp stair (green line) has the lowest elevation of +1.65 and the highest is +17.95, with a downstream water level elevation of +10.50. On average, the the negative stepp stair a higher water level, causing the flow velocity to be slower than the USBR Type III model.

CONCLUSION

From the test results on the hydraulic performance and effectiveness of the USBR Type III stilling basin and the the negative stepp stair, it can be concluded that:

1. The dissipation ratio produced by the model of the negative stepp stair is more optimal in reducing flow energy than the USBR Type III model. USBR Type III produces an average energy dissipation ratio of 69.47%. The ratio of energy dissipation generated by the model of the negative stepp stair is 67.30%.
2. The efficiency produced by the negative stepp stair model is greater than that of the USBR Type III model. The average efficiency produced by USBR Type III is 30.53%, while the efficiency produced by the negative stepp stair is 32.70%, an increase of 2.17%.
3. The velocity value of the negative stepp stair is below that of the USBR Type III model. The velocity in the USBR Type III model is 19.17 m/s–29.80 m/s, while in the negative stepp stair d it is 17.42 m/s–28.14 m/s.
4. The water level elevation in the USBR Type III has the lowest water level elevation of +1.65 and the highest is +16.95, with a downstream water level elevation of +10.50. The water level condition in the negative stepp stair has the lowest elevation of +1.65 and the highest at +17.95, with a downstream water level elevation of +10.50. On average, the negative stepp stair produces a higher water level.
5. It can be concluded that if the model of the negative stepp stair is applied later, it will reduce erosion symptoms downstream of the stilling basin due to the lower density that occurs.

Acknowledgements

The authors thank the Ministry of Education, Culture, Research and Technology (Higher Education Financing Center-BPPT) and the Institute of Educational Fund Management (LPDP) for supporting this research.

REFERENCES

[1] Aditya, R. F., Wahono, E. P., & Tugiono, S. (2021). Analisis Perbandingan Pola Aliran Pada Bangunan

Pelimpah Ogee Dan Stepped Dengan Model Fisik 2D. *JRSDD*, *9*(1), 41–50.

[2] Babaali, H., Shamsai, A., & Vosoughifar, H. (2015). Computational Modeling of the Hydraulic Jump in the Stilling Basin with Convergence Walls Using CFD Codes. *Arabian Journal for Science and Engineering*, *40*(2), 381–395. https://doi.org/10.1007/s13369-014-1466-z

[3] Bahmanpouri, F., Gualtieri, C., and Chanson, H. (2023). 'Experiments on two-phase flow in hydraulic jump on pebbled rough bed: Part 2–Bubble clustering', Water Sci. Eng., vol. 16, no. 4, pp. 369–380, doi: 10.1016/j.wse.2023.05.003

[4] Bantacut, A. Y., Azmeri, A., Jemi, F. Z., Ziana, Z., and Muslem, M. (2022). 'An experiment of energy dissipation on USBR IV stilling basin – Alternative in modification', J. Water L. Dev., vol. 53, pp. 68–72, doi: 10.24425/jwld.2022.140781.

[5] Barjastehmaleki, S. (2015). *Spillway Stilling Basins And Plunge Pools*. Trieste, Italy: Universit`a degli Studi di Trieste.

[6] Bradley, J. N., & Peterka, A. J. (1958). *Hydraulic Design of Stilling Basins and Energy Dissipators* (A Water Re, Vol. 84, Issue 5). Bureau Of Reclamation. https://doi.org/10.1061/jyceaj.0000243

[7] Chanson, H., & Brattberg, T. (2000). Experimental study of the air-water shear flow in a hydraulic jump. *International Journal of Multiphase Flow*, *26*(4), 583–607. https://doi.org/10.1016/S0301-9322(99)00016-6

[8] Daneshfaraz, R., Abbaszadeh, H., and Aminvash, E. (2022). 'Theoretical and Numerical Analysis of Applicability of Elliptical Cross-Section on Energy Dissipation of Hydraulic Jump', *Turkish J*. Hydraul. Theor., vol. 35, no. December, pp. 22–35.

[9] Dara Lufira, R., & Marsudi, S. (2015). Analisa Model Fisik Pelimpah Bendungan Sukahurip di Kabupaten Pangandaran Jawa Barat. *Jurnal Teknik Pengairan*, *6*, 14–21.

[10] Elnikhely, E. A., and Fathy, I. (2020). 'Prediction of scour downstream of triangular labyrinth weirs', Alexandria Eng. J., vol. 59, no. 2, pp. 1037–1047, 2020, doi: 10.1016/j.aej.2020.03.025.

[11] Gebhardt, M., Pfrommer, U., Rudolph, T., and Thorenz, C. (2018). 'Numerical and physical study on the energy dissipation at inflatable gates', 7th IAHR Int. Symp. Hydraul. Struct. ISHS 2018, vol. 26, pp. 174–183, doi: 10.15142/T3JD26.

[12] Hager, W. H. (1992). Energy dissipators and hydraulic jump. In *Journal of Fluid Mechanics* (1st editio, Vol. 247). Kluwer Academic. https://doi.org/10.1017/S002211209321062X

[13] Hassanpour, N., Dalir, A. H., Bayon, A. and Abdollahpour, M. (2021). 'Pressure fluctuations in the spatial hydraulic jump in stilling basins with different expansion ratio', Water (Switzerland), vol. 13, no. 1, pp. 1–15, 2021, doi: 10.3390/w13010060.

[14] Hendratta, L. A., & Tangkudung, H. (2020). *Hidraulika* (A. D. U. Press (ed.); Cetakan Pe). Unsrat Press.

[15] Ibrahim, M. M., Refaie, M. A., and Ibraheem, A. M. (2022). 'Flow characteristics downstream stepped back weir with bed water jets', Ain Shams Eng. J., vol. 13, no. 2, p. 101558, doi: 10.1016/j.asej.2021.08.003.

[16] Jayant, H. K. and Jhamnani, B., (2023) 'Numerical simulation of free and submerged hydraulic jump over trapezoidal and triangular macroroughness', Heliyon, vol. 9, no. 11, p. e22540, doi: 10.1016/j.heliyon.2023.e22540a

[17] Kurniati, Irwansyah, A., Irham, & Rosalina. (2019). Pengaruh Pasang Surut Terhadap Profil Aliran Muara Sungai Krueng Baro. *Portal: Jurnal Teknik SipilJurnal Teknik Sipil*, *10*(2), 1–6. https://doi.org/10.30811/portal.v10i2.973

[18] Kurniawan, F., & Siregar, G. G. P. (2022). Evaluasi Aliran Getar dan Kavitasi Pelimpah Bendungan Dolok. *Siklus : Jurnal Teknik Sipil*, *8*(1), 37–46. https://doi.org/10.31849/siklus.v8i1.7106

[19] Li, S., Li, Q., & Yang, J. (2019). CFD Modelling of a Stepped Spillway with Various Step Layouts. *Mathematical Problems in Engineering*, *2019*, 1–12. https://doi.org/10.1155/2019/6215739

[20] Mansoori, A., Erfanian, S., & Khamchin Moghadam, F. (2017). A Study of the Conditions of Energy Dissipation in Stepped Spillways with Λ-shaped step Using FLOW-3D. *Civil Engineering Journal*, *3*(10), 856. https://doi.org/10.28991/cej-030920

[21] Noverdo, R., Dermawan, V., & Sisinggih, D. (2021). Studi Eksperimen Kehilangan Energi Pada Sistem Pelimpah Dengan Kemiringan 1 : 1 Akibat Penurunan Dasar Kolam Olak. *Jurnal Teknologi Dan Rekayasa Sumber Daya Air*, *1*(1), 229–237. https://doi.org/10.21776/ub.jtresda.2021.001.01.20

[22] Pamungkas, E. J. W. (2014). Analisis Gerusan Di Hilir Bendung Tipe USBR-IV. *Jurnal Teknik Sipil Dan Lingkungan*, *2*(3), 389–396.

[23] Prasetyorini, L., & Priyantoro, D. (2015). Penggunaan Stilling Basin Tipe Bremen Modifikasi Pada Pelimpah Bendungan Tugu Di Kabupaten Trenggalek. *Jurnal Teknik Pengairan*, *6*(1), 116–124.

[24] Putro, H., & Hadihardaja, J. (2013). Variasi Koefisien Kekasaran Manning (n) pada Flume Akrilic pada Variasi Kemiringan Saluran dan Debit Aliran. *Jurnal Media Komunikasi Teknik Sipil*, *19*(2), 141–146.

[25] Qin, F., Tao, G., Liu, C., Wu, L., Qi, and Li, J., (2020). 'Comparative Study on Energy Dissipation Numerical Simulation of Different Energy Dissipators in Wide and Narrow Alternated Channels', IOP Conf. Ser. Earth Environ. Sci., vol. 526, no. 1, doi: 10.1088/1755-1315/526/1/012109.

[26] Rohmanto, H., Sawito, K., Siregar, H., & Tantular Jakarta, M. (2021). Analisis Pola Aliran Saluran Terbuka Dengan Hambatan Persegi Panjang, Bulat, Segitiga, Dan Wing. *Seminar Nasional Ketekniksipilan, Infrastruktur Dan Industri Jasa Konstruksi (KIIJK)*, *1*(1), 2021.

[27] Sasra Olga Pandani, M., Wahono, E. P., Chandra, R. W., & Mariyanto. (2022). Analisis Pola Hidraulik Peredaman Energi Pada Kolam Olak Tipe Vlughter Di Hilir Pelimpah Bertangga dengan Model Fisik 2D. *JRSDD*, *10*(1), 39–052.

[28] Soori, S., Babaali, H., and Soori, N. (2017). 'An Optimal Design of the Inlet and Outlet Obstacles at USBR II Stilling Basin', Int. J. Sci. Eng. Appl., vol. 6, no. 5, pp. 134–142, doi: 10.7753/ijsea0606.1001.

[29] Suroto Budinetro, H., Abdurrosyid, J., Ari Praja, T., & Sri Rahayu, D. (2010). A Spillway Structure with Stilling Basin Type Solid Roller Bucket and Baffle Block at Embung Wonosari. *Dinamika TEKNIK SIPIL*, *10*(3), 285.

[30] Tiwari, H. L. and Goel, A. (2014) 'Effect of End Sill in the Performance of Stilling Basin Models', Am. J. Civ. Eng. Archit., vol. 2, no. 2, pp. 60–63, 2014, doi: 10.12691/ajcea-2-2-1.

[31] Ulfiana, D. (2018). *Studi Efektivitas Pola Pemasangan Baffled Block pada Peredam Energi dalam Mereduksi Energi Aliran*. Unpublished Master's Thesis , Surabaya: Institut Teknologi Sepuluh Nopember.

[32] Valero, D., Bung, D., Crookson, B. M., & Matos, J. (2016). Numerical investigation of USBR type III stilling basin performance downstream of smooth and stepped spillways. *6th International Symposium on Hydraulic Structures: Hydraulic Structures and Water System Management, ISHS 2016*, *3406281608*, 635–646. https://doi.org/10.15142/T340628160853

[33] Vayghan, V. H., Mohammadi, M., and Ranjbar, A. (2019) 'Experimental Study of the Rooster Tail Jump and End Sill in Horseshoe Spillways', Civ. Eng. J., vol. 5, no. 4, pp. 871–880, 2019, doi: 10.28991/cej-2019-03091295.

[34] Wahl, T. L., and Falvey, H. T. (2022) 'SpillwayPro: Integrated Water Surface Profile, Cavitation, and Aerated Flow Analysis for Smooth and Stepped Chutes', Water (Switzerland), vol. 14, no. 8, doi: 10.3390/w14081256.

[35] Yusuf, M., & Wibowo, G. D. (2013). Pengaruh Pelimpah Bertangga Tipe Akar Terpotong Terhadap Panjang Loncatan Air Dan Kehilangan Energi Pada Kolam Olak. *International Conference on Infrastructure Development*, *1*(2008), 197–205.

[36] Zulfan, J. (2017). Hydraulic Optimization for Mitigating Local Scour Downstream of Weir (Case Study: Rengrang Weir, West Java). *Jurnal Teknik Hidraulik*, *8*(1), 15–28.

[37] Zulfan, J., Rakhmawati, T., Rimawan, R., Samskerta, I. P., & Lestari, S. (2022). Modifikasi Kolam Olak Tipe Ambang Bergigi Dalam Rangka Rehabilitasi Kerusakan Bendung Cikeusik Di Jawa Barat. *Jurnal Teknik Hidraulik*, *13*(1), 39–52. https://doi.org/10.32679/jth.v13i1.690